

# Earth's Future

## RESEARCH ARTICLE

10.1029/2019EF001169

### Key Points:

- Hydroclimatic parameters show a consistent pattern of change delineating four hydroclimate change regions
- Future African hydroclimate is likely to change with similar regional patterns regardless of the emission mitigation scenarios
- The Paris Agreement could limit the intensity of the hydroclimatic change but not the direction of the change

### Supporting Information:

- Supporting Information S1

### Correspondence to:

L. Piemontese,  
luigi.piemontese@su.se

### Citation:

Piemontese, L., Fetzer, I., Rockström, J., & Jaramillo, F. (2019). Future hydroclimatic impacts on Africa: Beyond the Paris Agreement. *Earth's Future*, 7, 748–761. <https://doi.org/10.1029/2019EF001169>

Received 29 JAN 2019

Accepted 15 MAY 2019

Accepted article online 7 JUN 2019

Published online 11 JUL 2019

Corrected 10 JUL 2020

This article was corrected on 10 JUL 2020. See the end of the full text for details.

©2019. The Authors.

This is an open access article under the terms of the Creative Commons Attribution-NonCommercial-NoDerivs License, which permits use and distribution in any medium, provided the original work is properly cited, the use is non-commercial and no modifications or adaptations are made.

## Future Hydroclimatic Impacts on Africa: Beyond the Paris Agreement

Luigi Piemontese<sup>1</sup> , Ingo Fetzer<sup>1</sup> , Johan Rockström<sup>1,2</sup> , and Fernando Jaramillo<sup>1,3,4</sup> 

<sup>1</sup>Stockholm Resilience Centre, Stockholm University, Stockholm, Sweden, <sup>2</sup>Potsdam Institute for Climate Impact Research, Potsdam, Germany, <sup>3</sup>Department of Physical Geography, Stockholm University, Stockholm, Sweden, <sup>4</sup>Baltic Sea Centre, Stockholm University, Stockholm, Sweden

**Abstract** Projections of global warming in Africa are generally associated with increasing aridity and decreasing water availability. However, most freshwater assessments focus on single hydroclimatic indicators (e.g., runoff, precipitation, or aridity), lacking analysis on combined changes in evaporative demand, and water availability on land. There remains a high degree of uncertainty over water implications at the basin scale, in particular for the most water-consuming sector—food production. Using the Budyko framework, we perform an assessment of future hydroclimatic change for the 50 largest African basins, finding a consistent pattern of change in four distinct regions across the two main emission scenarios corresponding to the Paris Agreement, and the business as usual. Although the Paris Agreement is likely to lead to less intense changes when compared to the business as usual, both scenarios show the same pattern of hydroclimatic shifts, suggesting a potential roadmap for hydroclimatic adaptation. We discuss the social-ecological implications of the projected hydroclimatic shifts in the four regions and argue that climate policies need to be complemented by soil and water conservation practices to make the best use of future water resources.

### 1. Introduction

Attaining the Sustainable Development Goal No. 2 of hunger eradication in Africa, the continent with the world's highest malnutrition (Bain et al., 2013), highest estimated population growth (Asongu, 2013) and severe water scarcity (Porkka et al., 2016) is a major challenge. Additionally, anthropogenic climate change is expected to further compromise water availability and food security in the next decades (Arnell, 2004; Rockström et al., 2017), considering that Africa is highly dependent on hydroclimatic resources (Collier et al., 2008) and has low adaptive capacity to these changes (Downing et al., 1997).

To prevent the negative consequences of climate change, the international community recently committed to constrain anthropogenic global warming within the Paris Agreement (UNFCCC, 2015), but the effectiveness of complying with the 2° target for African water resources is still debated (Easterly, 2009; Raftery et al., 2017). The reason is that, to date, there is no comprehensive assessment of the impact of different climate change scenarios on African water resources. In fact, model-based assessments usually rely on separate analysis on hydroclimatic parameters such as precipitation (P; Giorgi et al., 2014) or runoff (R; Boko et al., 2007; Goulden et al., 2009; Nohara et al., 2006), commonly used to measure water availability (Faramarzi et al., 2013; Mekonnen & Hoekstra, 2016). For P, climate projections foresee a general decrease over Northern and Southern Africa and increase in the equatorial region and the Sahel (Huntington, 2006; Karl & Knight, 1998). In relation to R, some studies predict a decrease over Southern Africa (Hagemann et al., 2013; Vörösmarty et al., 2000), increase over eastern equatorial Africa (Schewe et al., 2014; Vörösmarty et al., 2000) and potential severe water stress—defined as total water demand over runoff—in North Africa, Sahel, Horn of Africa, and South West Africa during the first half of the current century (Milly et al., 2005). In addition, climate models also show a ubiquitous decreasing trend in soil moisture (Sm) in the coming decades (Sheffield & Wood, 2008). These hydroclimatic changes may affect crop production, putting an extra burden on countries where migration of famine refugees has caused conflicts and social tensions (Nnoli, 1990). However, the high uncertainty related to the projections of P, R, and Sm (Scheff & Frierson, 2015; Teng et al., 2012) calls for an increased effort in hydrological assessment to provide more consistent estimates of future hydroclimatic trajectories. In fact, hydroclimatic impacts based on only one parameter (e.g., P or R) are highly conditioned by the resolution and reliability of the models to capture

the specific physical processes related to that parameter (Sylla et al., 2013), while the assessment based on multiple hydroclimatic parameters can reduce this uncertainty (Trenberth et al., 2003). Another major limitation with assessments based on single hydroclimatic parameters is that they do not consider cumulative effects (e.g., what happens if R increases and Sm decreases simultaneously?) providing partial information that can cause misleading interpretation and uninformed planning (Dai, 2011a, Hirabayashi et al., 2008).

What determines water availability for food production and ecosystems, particularly on the African continent where >95% of agriculture is rainfed (Schuol et al., 2008), is the net amount of water in soils after subtracting loss of water due to evaporation. In this context, hydroclimatic assessments, looking at the combined effect of changes in P, potential evapotranspiration (PET), and actual evapotranspiration (E; Weiskel et al., 2014; Scheff & Frierson, 2015), can better describe the overall effect of climate warming on the hydroclimate (Bring et al., 2015; Gudmundsson et al., 2017; Huntington, 2006). In fact, over long time scales, the partitioning of water between R and E is controlled by water and energy availability in terms of P and PET (Budyko, 1971). PET depends on energy among other factors, and it is expected to increase with global warming as temperatures rise (Morsy et al., 2016), modifying the patterns, magnitude, and seasonality of P (Dore, 2005), with unclear effects on aridity and water partitioning. For instance, in regions where the increase in P is less relevant than the increase in PET, the net water balance would lead to an increase in aridity conditions (aridification; see Sherwood & Fu, 2014); however, the assessment based on changes in P only would predict increasing water availability leading to potential misinterpretations.

In this work, we use the Budyko framework (Budyko, 1963) to provide a comprehensive hydroclimatic assessment of the impact of the two main Representative Greenhouse Gas Concentration Pathways (RCPs)—the Paris Agreement (RCP4.5) and the business as usual (RCP8.5). The RCPs are climate projections forced with distinct greenhouse gas concentrations, generally covering the period 2006–2099. The RCP4.5 corresponds to the midrange mitigation emission scenario adopted by the Paris Agreement, while the RCP8.5 represents the highest emission rate from a business as usual scenario—a scenario without any emission mitigation strategy.

The Budyko framework provides a relationship between the aridity index (PET/P) and the evaporative ratio (E/P). As such, we refer to the mathematical space generated by PET in the  $x$  axis and E/P on the  $y$  axis as the Budyko space. Looking at the ratios between the key water and energy balance parameters can give a general insight on the main wetting and drying trends (Greve et al., 2014), linking changes in energy demand driven by climate warming to resulting effects on water partitioning and water availability on land. We first use the multimodel ensemble data from nine Earth system models (ESM) within the CMIP5 project (Taylor et al., 2011) that have simultaneous fine-scale data on temperature ( $T$ ), P, R, E, and Sm to characterize in the Budyko space the aridity and water partitioning conditions in the 50 largest African basins. Second, we compare the hydroclimatic changes expected for both scenarios, here referred to the changes in the main hydroclimatic parameters (P, R, E, Sm, PET/P, and E/P). Finally, we cluster African basins into four hydroclimate change groups, highlighting potential implications for human and agricultural activities. This classification may be used by water-related stakeholders to understand the main trade-offs and synergies of forthcoming hydroclimatic change and water management and to plan sustainable strategies for eradicating hunger in Africa.

## 2. Data and Methods

To investigate the impacts of the two RCPs—RCP4.5 and RCP8.5—on African hydroclimate, we calculate hydroclimatic changes between the periods 1960–1989 and 2070–2099 for the RCPs and the historical experiment. The historical experiment consists of a set of simulations forced by observed atmospheric conditions from both natural and anthropogenic sources—including land cover modifications—covering the whole twentieth century.

We used simulations from nine ESM (models' characteristics in supporting information Table S1) within the Coupled Model Intercomparison Project (CMIP5). The CMIP5 simulations have been used in previous studies for direct calculation of hydrological fluxes in basins greater than 10,000 km<sup>2</sup> without necessary downscaling (Asokan et al., 2016; Bring et al., 2015; Flint & Flint, 2012). In the model selection process, we excluded the lower-resolution models (>2.5° resolution) because of their poor performance when

reproducing T, P, and E for Africa (Bhattacharjee & Zaitchik, 2015; Kharin et al., 2007; Siam et al., 2013). Nine is the maximum number of CMIP5 models providing all the variables used in this study. The variables taken from the CMIP5, (with their original database names in brackets) are total soil moisture content (mrso), runoff (mrro), specific humidity (hus), surface downwelling shortwave radiation (rsds), air temperature (ta), precipitation (pr), evapotranspiration (evpbs), and surface air pressure (ps)—for the three experiments analyzed (“historical,” “RCP4.5,” and “RCP8.5”). The reason of the (relatively) limited number of models used in this study is because usually multimodel ensemble studies focus on the atmospheric component of ESM. The atmospheric component is the most common and well studied within the CMIP5 project, so a large number of models provide simulations for atmospheric variables (e.g., precipitation and radiation). Unfortunately, not all ESM have a complex land system component, which is the one computing soil moisture and (in most cases) runoff. Since our study aims at providing a comprehensive analysis on the main component of the water cycle interacting with climate, only nine models could provide the necessary atmospheric and land system variables for the three experiment used in our analysis.

Since climate simulations are dependent on their initial state (i.e., the values of some physical parameters set to represent the climate variability), the CMIP5 models produce ensembles of simulations with different initializations to capture the natural climate variability, called realizations. In our analysis, the realization r1i1p1 (r: realization, i: initialization, and p: perturbation) was used, in analogy with other studies (Bring et al., 2015), because it provides the largest number of simulations.

Geospatial data of African basins were derived from the Global Runoff Data Centre (2017). We first selected the basins with surface areas larger than 10,000 km<sup>2</sup> (53 in total) to deal with the coarse resolution of some models' outputs. We later excluded some river basins such as the Doring in South Africa, Sebou in Morocco, and Lake Turkana in East Africa, because not all the models could cover their extent given their coarse resolution. Hence, the final number of basins analyzed in this study became 50, covering the 62.2% of the total African surface. The 50 basins are located mostly in sub-Saharan Africa, leaving only small coastal basins and desert areas (e.g., Namibia and the horn of Africa) out of the basin coverage.

### 2.1. Estimation of PET

Because estimation of aridity may be very sensitive to the methods behind the calculation of PET (Milly & Dunne, 2016; Seneviratne, 2012), we computed PET in two different ways: the open water Penman-Monteith PET, here referred to as PET<sub>OW</sub> (Dai, 2013; Donohue et al., 2010; Sheffield et al., 2012), and the energy-only PET suggested by Milly and Dunne (2016) and used specifically for CMIP5 model outputs, here referred to as PET<sub>EO</sub> (Milly & Dunne, 2016). We calculated the average of the two different methods to estimate mean PET at the basin scale. The two PET equations are the following:

$$PET_{OW} = \frac{\Delta}{\Delta + \gamma} (R_n - G) + \frac{\gamma}{\Delta + \gamma} \frac{6.34(1 + 0.536u)(e_s - e)}{L_v}, \quad (1)$$

$$PET_{EO} = 0.8(R_n - G), \quad (2)$$

where  $R_n$  (mm/day) is the net radiation;  $u$  (m/s) and  $G$  (mm/day) are the wind speed at 2-m height and the heat flux into the subsurface, respectively. The values of  $u$  and  $G$  were set to 1 and 0, respectively, as PET has been previously tested on these parameters and found to be largely insensitive to their variations (Cook et al., 2014). The term 0.8 of the PET<sub>EO</sub> equation represents the fraction of available energy that goes into latent heat flux (Milly et al., 2016), estimated by Koster and Mahanama (2012) to be about 80% based on observation-model analysis.

The  $L_v$  is the latent heat of vaporization of water (MJ/kg), given by

$$L_v = 2.501 - 0.002361T, \quad (3)$$

where  $T$  (°C) is air temperature at 2-m height;  $e$  (kPa),  $e_s$  (kPa), and  $\Delta$  (kPa/K) are the vapor pressure at 2 m (equation (4)), the saturation vapor-pressure function (equation (5)), and its derivative with respect to  $T$  (equation (6)), respectively, while  $\gamma$  (kPa/K) is the psychrometric constant (equation (7)).

$$e = \frac{Pq}{0.622 + 0.378q} \quad (4)$$

$$e_s = 0.6108 \exp\left[\frac{17.27T}{T + 273.3}\right] \quad (5)$$

$$\Delta = \frac{4098e_s}{(T + 273.3)^2} \quad (6)$$

$$\gamma = 0.000665P \quad (7)$$

## 2.2. Analysis of Hydroclimatic Change in the Budyko Space

We analyzed changes in PET/P and E/P within the Budyko hydroclimatic framework to describe the future trends in aridity and water partitioning. The Budyko framework describes the relationship of the partitioning of water and energy on land, considering that evapotranspiration is limited by the availability of water (i.e., P) and energy (i.e., PET). The relationship between PET/P and E/P has been analytically described by a set of Budyko-type equations (e.g., Choudhury, 1999; Yang et al., 2008) expressing E/P as a function of PET/P. For example, the “Budyko-type” formulation of Yang et al. (2008) is a climatic model of E/P in terms of PET/P and other parameters representing the effect of basin characteristics, such as vegetation, soils, and topography. A basin that changes its hydroclimatic conditions from a period 1 ( $p_1$ ) to a period 2 ( $p_2$ ) can be represented in Budyko space by a point moving from the initial conditions  $p_1$  to the final conditions  $p_2$  (Figure S1). These conditions should be constrained to the limits  $E/P < 1$ ,  $E/P > 0$ , and  $E/P < PET/P$ . Under the hypothetical condition that the changes in PET/P are the only drivers of change in E/P, the basin will move to a new location along the Budyko-type curve representing the characteristic initial climatic and catchment conditions. However, in a more realistic scenario where E/P depends not only on changes in PET/P but also on other drivers in the landscape, the basin can move anywhere in Budyko space (van der Velde et al., 2014).

We then define the total hydroclimatic change experienced by any basin over time as the movement vector ( $\vec{h}_s$ ) in the Budyko space between the two points representing the initial and final hydroclimatic conditions of the basin. As such, the horizontal component of the movement vector is the difference between the 30-year annual means of PET/P of the periods 1960–1989 and 2070–2099,  $\Delta$  (PET/P), and the vertical component the difference between the 30-year annual means of E/P of the periods 1960–1989 and 2070–2099,  $\Delta$ (E/P). These periods have been often selected to study the future hydroclimatic conditions of a given basin and its corresponding change (Bring et al., 2015; Feng & Fu, 2013).

The intensity of the total movement ( $I_s$ ) is the magnitude of the vector, and the direction ( $\theta_s$ ) is the clockwise angle between  $\vec{h}_s$  and the positive y axes, as follows:

$$I_s = |\vec{h}_s| = \sqrt{\Delta\left(\frac{PET}{P}\right)^2 + \Delta\left(\frac{E}{P}\right)^2}, \quad (8)$$

$$\theta_s = b - \left( \text{atan2} \frac{\left(\Delta\left(\frac{E}{P}\right)^2, \Delta\left(\frac{E}{P}\right)^2\right) * 180}{\pi} \right), \quad (9)$$

where  $b = 450^\circ$  when  $\Delta$ (E/P) > 0 and  $\Delta$  (PET/P) < 0, and  $b = 90^\circ$ .

We used this vector representation to depict the movements of the 50 largest African basins in the Budyko space, visualized by a wind rose diagram. Wind rose plots aggregate information on intensity, direction, and frequency of the movement. This type of diagrams has been used in global (Jaramillo & Destouni, 2014, 2015) hydroclimatic change assessments. We used this approach to depict simultaneously the hydroclimatic movement in the Budyko space for the 50 largest African basins for both the RCP4.5 and RCP8.5, following Jaramillo and Destouni (2014). All the basins with movements in Budyko space in a particular range of direction are grouped in a petal.

### 2.3. Identification of Future Hydroclimate Change Regions

To infer possible regional patterns of future hydroclimatic change, we clustered the basins in four main groups according to their current aridity conditions and their forecasted change in PET/P, E/P, P, and Sm. We first classified the basins in two main aridity classes using the average value of the PET/P in the period 1960–1989 as measure of aridity. Because of the diverse—and inconsistent—approaches used to delineate the boundaries between aridity classes (Gamo et al., 2013; Maliva & Missimer, 2012; Thornthwaite, 1948), we here used a simple method to split our group of basins in two major aridity groups, those tending to arid conditions and those to humid ones. As a threshold, we used the median PET/P value of the 50 African basins (PET/P = 2.4) to have a comparable number of basins in both aridity classes, so that the basins with condition PET/P > 2.4 were classified as arid and the remaining (i.e., PET/P < 2.4) as humid. The value 2.4 is a suitable threshold because it falls in the transitional semiarid group ( $2 \leq \text{PET/P} < 5$ ) of the United Nations Educational, Scientific and Cultural Organization (UNESCO) classification of climate zones based on aridity index (Barrow, 1992).

For each aridity group we then performed a hierarchical cluster analysis to identify the possible future hydroclimate change groups. Since we were interested in grouping basins with the same overall profiles regardless of their magnitudes, we used the Pearson correlation-based distance as a dissimilarity measure. The correlation-based distance considers two objects similar if their features are highly correlated, even though the observed values may be far apart in terms of Euclidean distance. This is the case of our hydroclimate change assessment, where we want to consider basins as “similar” if their hydroclimatic parameters (e.g., P or R) increase or decrease all together. Each resulting group represents a region with a coherent change in the hydroclimatic parameters relevant for African water availability (i.e., PET/P, E/P, P, and Sm), with distinctive implications for water resources management and specific social-ecological issues.

## 3. Results

### 3.1. Future Hydroclimatic Change Scenarios

The initial hydroclimatic conditions of the 50 African basins show a close resemblance between the spatial distributions of the aridity (i.e., PET/P) and water partitioning on land (i.e., E/P) throughout the continent (Figure 1). The initial aridity conditions in Africa from our analysis well reflect the pattern of previous estimates, showing a generally wetter condition in Congo and the western tropical coast (Zomer et al., 2008). Basins located in the Northwestern Africa and on the Sahel are arid, and precipitation is mostly partitioned into evapotranspiration (i.e., PET/P > 4 and E/P > 0.9), especially in the Chelif, Senegal, Gambia, and Lake Chad River Basins. In Southern Africa, especially the basins in the countries of Namibia and South Africa show equally high evaporative ratios as those of Northern Africa (i.e.,  $0.9 < \text{E/P} < 1.2$ ) although not as high aridity values ( $2 < \text{PET/P} < 3$ ). On the other hand, the tropical strip is the most humid region, with precipitation partitioned mostly into runoff, most notably in the west coast of Central Africa, where basins like Cross and Sanaga have low evaporative ratios (i.e.,  $0.6 < \text{E/P} < 0.7$ ).

Our analysis shows differences in expected hydroclimatic change between the two development pathways (Figure 2, summarizing the changes in E/P and PET/P from the period 1960–1989 to the period 2070–2099). In the RCP4.5 scenario, PET/P increases in 90% of the analyzed basins, while E/P shows much smaller changes when compared to those in PET/P. The RCP8.5 scenario shows more varied hydroclimatic changes among basins, with about 40% of the basins increasing PET/P (20% with intensity of the shift >0.3) and a range of basins with simultaneous decreasing PET/P and E/P. This trend agrees with the generic behavior described by the relation between E/P and PET/P in the Budyko Framework, where basin movements are more likely to occur in the directions represented by the upper-right or lower-left quadrants of the rose diagram (Gudmundsson et al., 2016; Yang et al., 2008).

On the contrary, movements in the direction of the lower-right quadrant, corresponding to increasing PET/P and decreasing E/P, and in the upper-left quadrant (decreasing PET/P and increasing E/P) account for almost 40% of the basins under the RCP4.5 scenario but less than 5% under RCP8.5. As such, changes in the partitioning of water into E and R for the RCP8.5 agree more with the expectations from the Budyko-type empirical models than for the RCP4.5, highlighting the driving role of the atmospheric water supply and energy availability on future water partitioning.

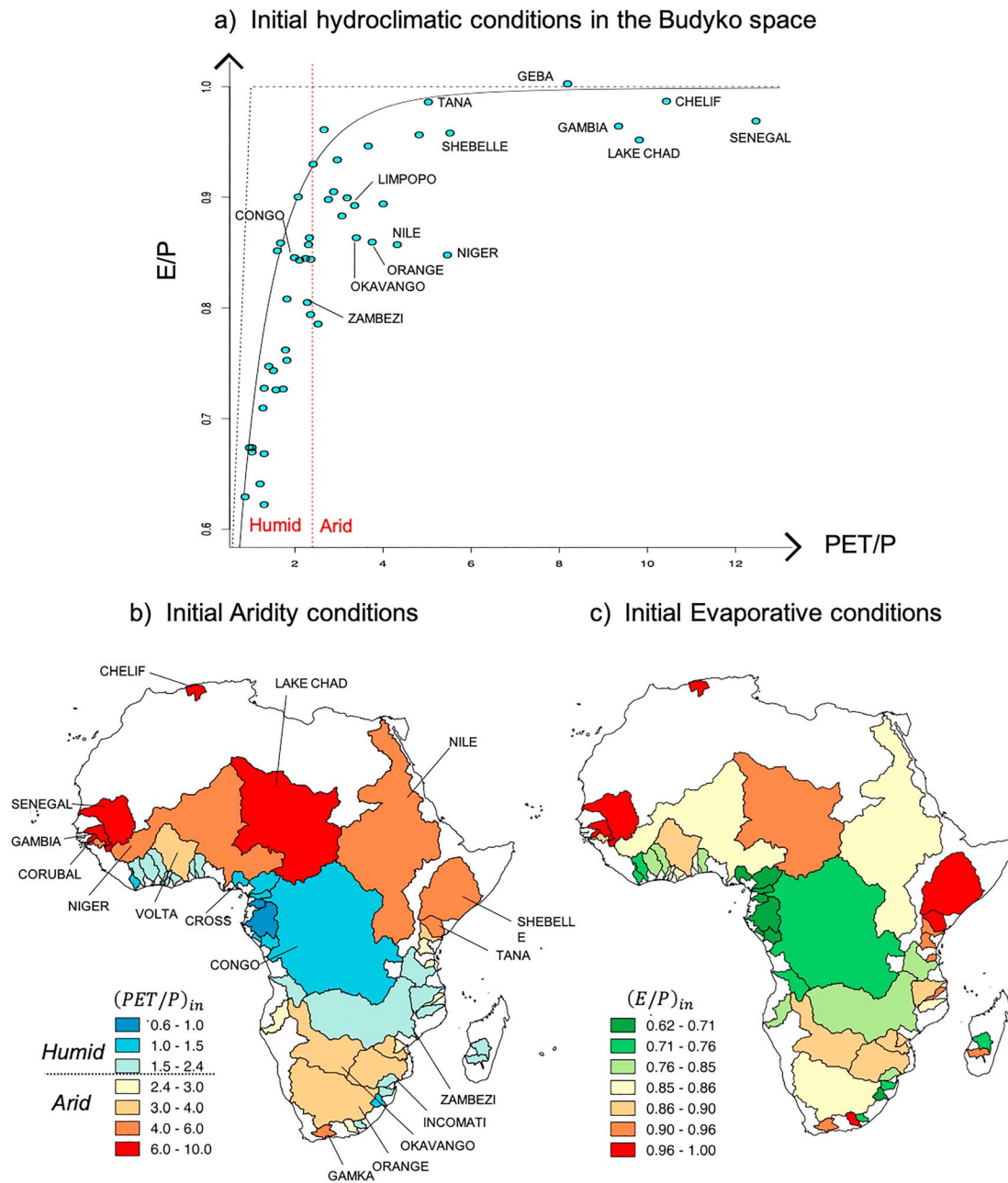


**Figure 1.** (a) Initial hydroclimatic conditions of the 50 largest African basins represented in Budyko space and given by the mean 30-year values of the aridity index (PET/P) and evaporative ratio (E/P) for the period 1960–1989. Maps of (b) the mean aridity index (PET/P) and (c) evaporative index (E/P).

### 3.2. Regional Patterns of Future Hydroclimatic Change in Africa

To understand the implications of hydroclimatic changes depicted in the roses (Figure 2), we performed a hierarchical cluster analysis on the average changes in E/P, PET/P, P, and Sm separately for arid (PET/P > 2.4) and humid (PET/P < 2.4) basins (see Figures S2 and S3 for detailed dendrograms). The results suggest that four different groups of basins can represent the patterns of hydroclimatic change for both the RCP4.5 and RCP8.5 scenarios in Africa (Figures 3 and S4). The error bars indicate the standard deviation—the spread between the average value and the nine ESM—which gives an indication of the agreement between the nine models. Overall, the agreement is lower for R and particularly low for Sm simulations, which are the most uncertain with only 10% of the basins showing a statistically significant change ( $p < 0.05$ ). The hydroclimate change group 1 shows the most reliable predictions given the highest number of significant

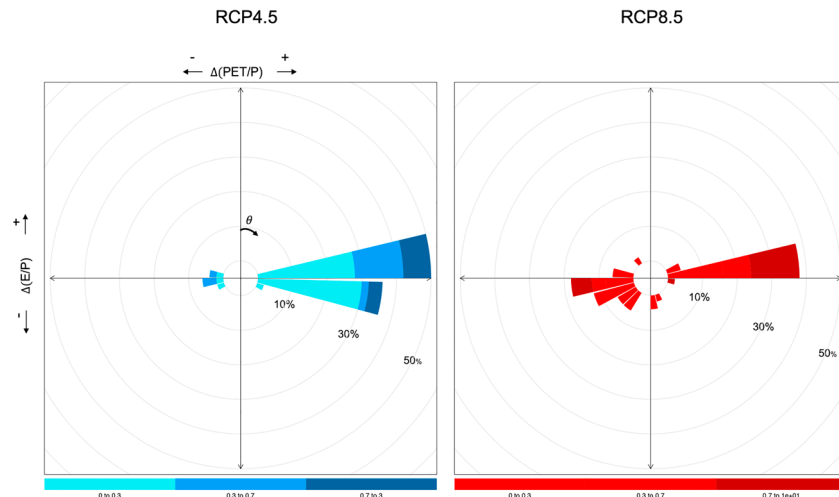


**Figure 2.** Roses of movement in Budyko space for the 50 basins represented as the combined changes in PET/P (horizontal axis) and E/P (vertical axis), between the 30-year means of the periods 1960–1989 and 2070–2099 for the RCP4.5 (blue) and RCP8.5 (red) scenarios. Each petal includes the basins moving within a range of directions of 15°, with directions  $\theta$  starting from the vertical axes and counterclockwise. The size of the paddle indicates the percentage of basins moving in that direction  $\theta$ . The intensity of the color indicates the intensity of the movement in the Budyko space in a given direction  $\theta$ .

changes across all the hydroclimatic parameters. Moreover, the pattern of change is fairly consistent across the two emission scenarios, with all the basins falling into the same groups in both scenarios, with the exception of the three arid basins in East Africa, Ruvu, Pangani, and Messalo, which cluster into group 1 in the RCP4.5 (Figure S4) and in group 2 in RCP8.5 (Figure 3).

The basins for each group are spatially distributed in a way that enables a clear delineation of the four regions depicted in Figure 4, regardless of the scenario. More specifically, group 1 (dark red group in the

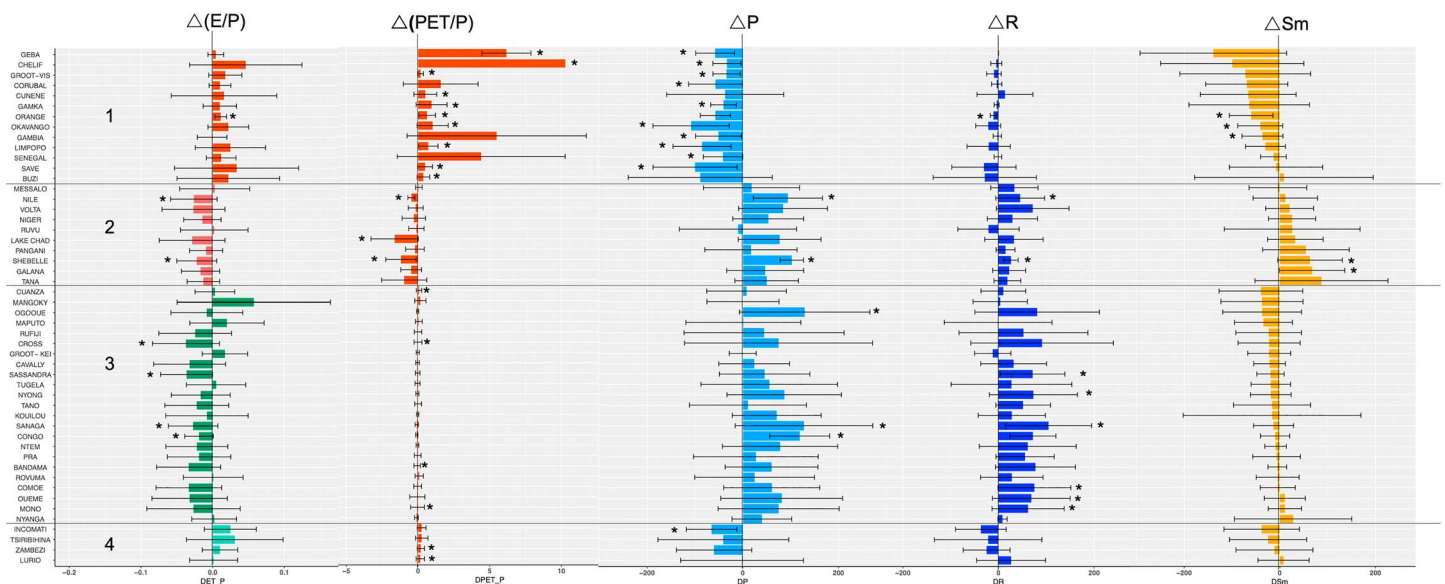


**Figure 3.** Bar plot showing the pattern of change in the main hydroclimatic parameters of evaporative ratio, E/P; aridity index, PET/P; precipitation, P; runoff, R; and soil moisture, Sm, from 1960–1989 to 2070–2099 for the RCP8.5 scenario. P, E, R, and Sm were derived from climate models' outputs, and PET is the average of two different methods (see section 2). Error bars represent the spread between the nine ESM and statistically relevant changes (Pearson;  $p < 0.05$ ) are marked with asterisks. The colors of the different parameters are chosen for visual purpose and are consistent throughout the paper. The colors of  $\Delta(E/P)$  represent the four clusters of hydroclimatic change used from now on—dark red for group 1 (for arid basins becoming more arid), light red for group 2 (for arid basins becoming wetter), dark green for group 3 (for humid basins becoming wetter), and light green for group 4 (for humid basins becoming drier).

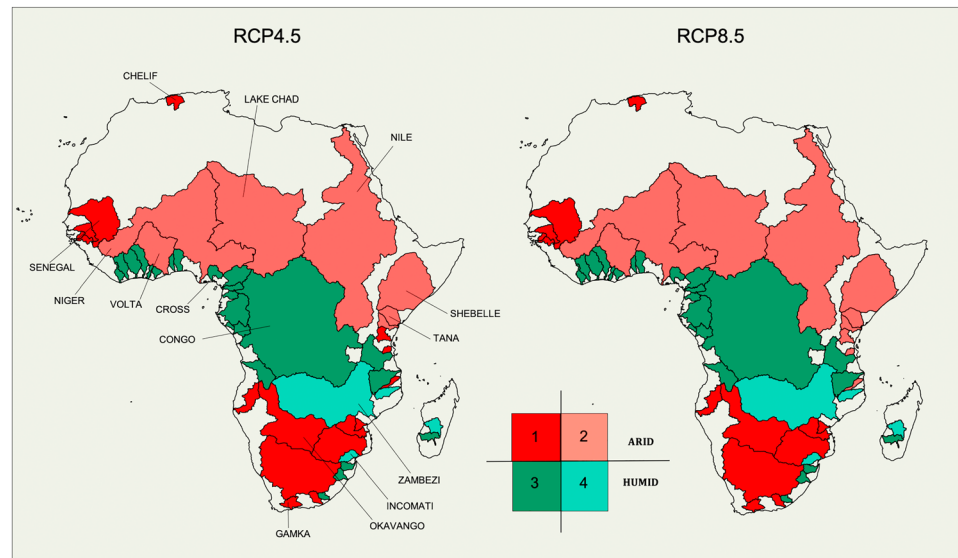


**Figure 4.** Map of African basins clustered according to the four future hydroclimate change regions for RCP4.5 (a) and RCP8.5 (b). The four groups emerge from the hierarchical cluster analysis accounting for changes in E/P, PET/P, P, and Sm in humid ( $PET/P < 2.4$ ) and arid ( $PET/P > 2.4$ ) basins separately.

following figures) includes five of the most arid basins in Northwestern Africa and the arid basins in Southern Africa, likely to experience a marked increase in aridity and a decrease in P, R, and Sm. Group 2 (light red) includes the Sahel strip and three of the largest African basins—Niger, Chad, and Nile—and it is characterized by decreasing aridity, resulting in a shift toward increasing P, R, and Sm. Group 3 (dark green), including mainly humid basins in tropical Africa, will experience increasing P and R without significant change in aridity conditions, leading to a slight decrease in Sm. Finally, group 4 (light green) is located in Southeastern Africa and embraces four humid basins, including the Zambezi River. These basins will experience a slight increase in aridity and a decrease in P, R, and Sm.

#### 4. Discussion

Regardless of the future emission trajectory, the 50 largest African basins are likely to experience a similar hydroclimatic direction of change in Budyko space as outlined in the four hydroclimate change groups. The difference in the two scenarios resides mainly in the intensity of the change (although disagreement between models is large) and the dominance of change in P and PET as drivers of changes in water partitioning, both stronger in the business as usual scenario (RCP8.5) when compared to the Paris Agreement one (RCP4.5).

In our basin-scale assessment, precipitation and runoff show a decreasing trend in the northern and southern regions of the continent (groups 1 and 4) and an increasing trend in tropical Africa and the Sahel (groups 2 and 3), which corroborates the results of previous studies (Dai, 2011a, 2011ab; Milly et al., 2005). With the exception of group 2, soil moisture shows mostly a downward trend in RCP8.5. The change in PET/P is a critical factor to interpret these changes. The PET/P trends in our results are in line with the widespread scientific opinion of the aridification of Southern and Northern Africa for both RCPs (Dai, 2011a, 2011ab; Feng & Fu, 2013; Fu & Feng, 2014; Scheff & Frierson, 2015). However, our results highlight a decrease in PET/P over the Sahel region (group 2), which can be the main driver of increasing soil moisture. Similarly, the moderate increase of PET/P in group 3 could explain the decrease of soil moisture despite the increase in precipitation and runoff, discussed further in detail.

The expected hydroclimatic changes for Africa can produce mixed effects on water resource management, potentially exacerbating water scarcity in the most critical regions of dry North and Southern Africa, whereas bringing potential benefits to food production and natural vegetation in the Sahel, currently experiencing a greening phase (Herrmann et al., 2005). The hydroclimate change regions are presented in

combination with some relevant agriculture-related socioeconomic indicators in Figure S5 to provide further guidance for understanding the social-ecological implications in the key African countries.

Group 1 (dark red basins in Figures 3–5) covers the arid regions of Northwestern and most of Southern Africa, dominated by pastoral lands and extensive cropping systems. These regions are likely to experience a marked increase in aridity and a decrease in long-term P, R, and Sm. This group includes Algeria and South Africa, which are the countries with the most intensive use of irrigation (You et al., 2011) and currently the most affected by water scarcity in the continent (Hoekstra et al., 2012). The projected hydroclimatic changes will increase the need of irrigation on one hand and decrease the availability of water for agriculture on the other hand, thus increasing the pressure on groundwater resources and potentially damaging agricultural productivity in both rainfed and irrigated fields. Another hotspot country is Mali, where extensive agriculture, supporting over 30% of the national gross domestic product (GDP), is concentrated in the Senegal basin, which will experience a decrease in precipitation and a marked increase in aridity. This long-term scenario appears heavily unsustainable for natural vegetation and human life, especially considering that the African population is expected to double by 2050 (Gerland et al., 2014). The widespread aridification underlines the need to implement agricultural practices able to cope with high PET in a context of reduced water availability. Basins in this group would benefit from practices such as (i) mulching and intercropping to avoid rapid soil evaporation, (ii) terracing to increase infiltration and increasing soil moisture, and (iii) rainwater harvesting techniques to make the best use of the scarce and seasonal precipitation. These practices are particularly effective in contrasting desertification in the arid and semiarid fringes of Senegal and Namibia, where combined intercropping and mulching increased crops yield considerably (Oweis & Hachum, 2006; Trail et al., 2016). Nevertheless, the rate of adoption of these practices among farmers is still low (Kahinda et al., 2008).

The second group (light red) embraces pastoral land and extensive cropping systems in the Sahel strip, characterized by arid basins with a projected increase in P resulting in increasing R and Sm. The Sahel is a region suffering from drought and famine, with large amount of undernourished population (58% in Central African Republic and 39% in Uganda with 39% and between 32.5% in Chad, 26% in Sudan, and 29% in Ethiopia). The economy of these countries is strongly dependent on agriculture (up to 51% of total GDP in Chad and Central African Republic) despite the current low crop yield. Crop production in the Sahel has a great potential for improving yields through irrigation (Jägermeyr et al., 2016), and it could benefit from increasing P and R. However, the presence of some of the largest African transboundary basins (Niger, Chad, and Nile) could rise upstream-downstream conflicts in water resources management, as has already happened between Ethiopia, Sudan, and Egypt over the Nile River (Swain, 2011). In fact, in these countries, barren lands and pastoral systems dominate the landscape and agriculture is heavily dependent on freshwater resources near rivers. Moreover, other trade-offs in water use might emerge between irrigation, urban water supply, and energy production—for example, hydropower, which is gaining popularity in Ethiopia (Bartle, 2002). In this context, the increase in P could represent a good opportunity to improve food production if properly harvested. For instance, water harvesting practices can be effectively used to increase water productivity in rainfed agriculture, increasing the yield without affecting downstream regions (Dile et al., 2016; e.g., Egypt), thus saving freshwater resources for other activities.

Group 3 (dark green) comprises the tropical forests of Central Africa, including the Congo and some coastal areas of Central and Western Africa. This group will experience an increase in precipitation and a slight increase in PET/P that will result in higher R in tropical humid/subhumid basins. The increasing P could benefit rainfed crop production in countries as Ivory Coast, Benin, and Togo where agriculture covers more than 70% of the land and has a strong influence on the economy (around 30% of GDP). However, the additional precipitation could likely come from stronger tropical cyclones (Knutson et al., 2010), thus increasing the R to P ratio and explaining the expected decrease in Sm. In fact, steady moderate P infiltrates more easily into the soil, increasing Sm, while the same amount of P concentrated in shorter periods causes higher R (possibly flooding) leaving soils eventually much drier (Trenberth et al., 2003). The same mechanism is also likely to promote nutrient loss because of the washout of the topsoil layer during extreme events, with negative consequences for agricultural productivity as already observed in the Congo basin (Few et al., 2014). National authorities should consider strengthening flood risk prevention plans, particularly in view of the expanding urban settlements. On the agricultural side, terracing and other slope control measures can prevent soil erosion and increase infiltration. Positive examples of these practices can be found across different

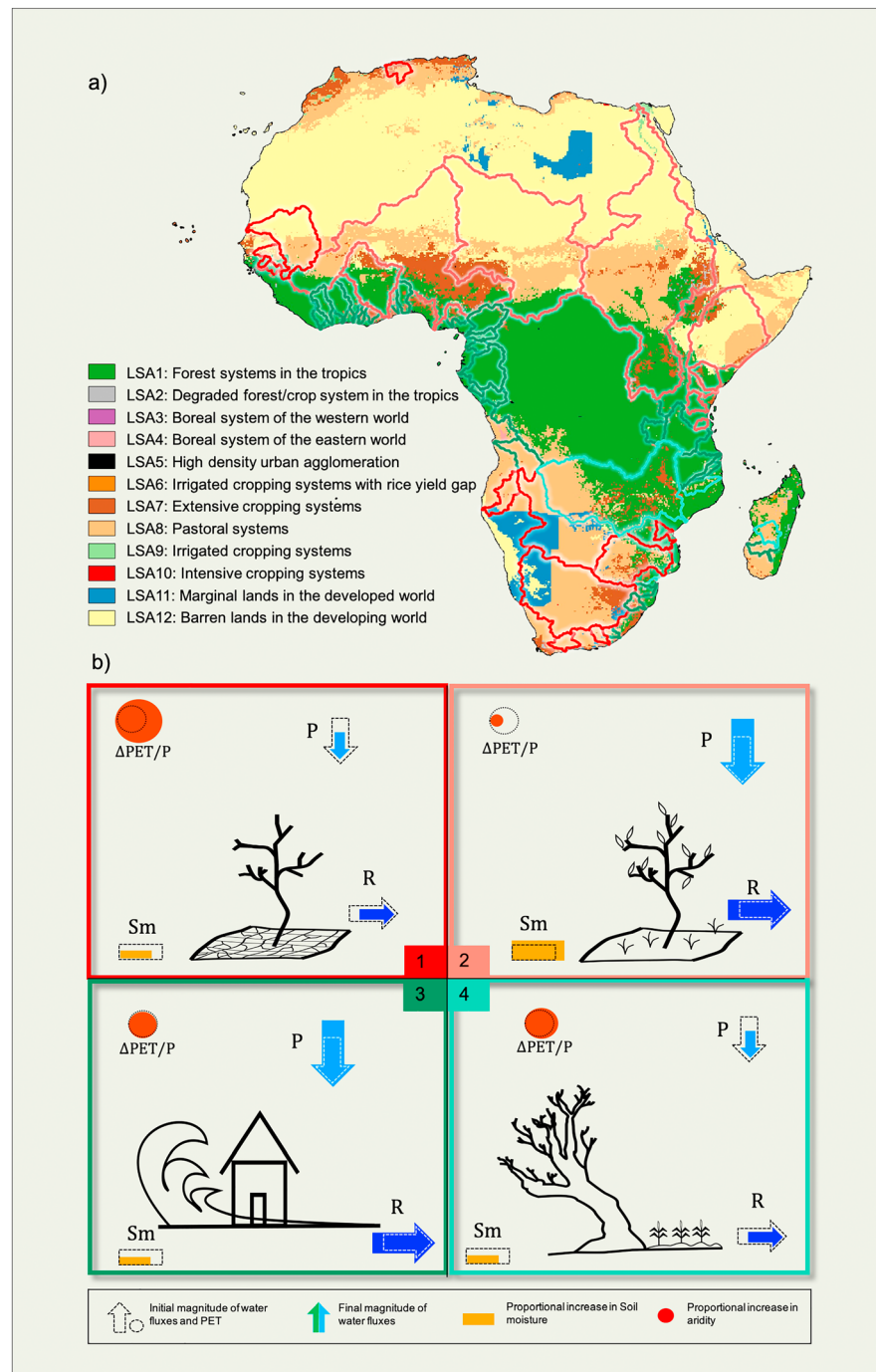


**Figure 5.** Implications of hydroclimatic changes for future water resources in Africa. The map (a) shows the 50 African basins divided in the four hydroclimate change groups in the RCP8.5 (as in Figure 4) overlaid to the land system archetypes (LSAs) map developed by Václavík et al. (2013). The LSA synthesizes the main social-ecological systems in Africa. The panel (b) is a graphic synthesis of the future hydroclimatic changes in Africa. The relative magnitude of water fluxes is depicted for precipitation (P), runoff (R), soil moisture (Sm), and aridity (PET/P) between the periods 1960–1989 (dashed) and 2070–2099 (colored). The four groups are the outcome of the cluster analysis, combining initial aridity conditions (PET/P < 2.4 and PET/P > 2.4) with the two sets of changes in PET/P, E/P, P, and Sm foreseen in Africa. The icons in the four groups serve to illustrate the potential implications of changes in hydroclimatic parameters on African social-ecological systems.

social-ecological context of Uganda, Rwanda, and Burundi (Liniger et al., 2002; WOCAT, 2017), where slope control measures helped contrasting excessive R and increasing Sm, leading to increased crop production and food security.

The last group (light green) includes six humid Southern African basins (e.g., the Zambezi River basin) with a projected increase in PET/P and decrease in P, R, and Sm. These hydroclimatic changes will result in less water available for both natural vegetation and rainfed agriculture in inland areas, with a particularly negative impact on the vast semiarid grasslands. These grasslands are most dependent on precipitation resources for vegetation growth and ecosystem's health (Weltzin et al., 2003). Grazing activities could put further pressure on rangelands increasing the risk of desertification triggered by increasing aridity. The Zambezi, for instance, is one of the largest rivers flowing on semiarid lands, making social-ecological systems notably dependent on its seasonal flooding cycles. The projected decrease in R could thus reduce or change flooding patterns, threatening the rich biodiversity of its delta, closely dependent on river discharge. Zambia represent a particularly sensitive situation, with 46% of undernourished population, but with an increasing crop production that may be at severe risk from hydroclimatic change. It is important to notice that in this group, the intensity of the hydroclimatic changes is essentially identical in both RCPs, suggesting that CO<sub>2</sub> emission reduction policies alone might not be enough to prevent the negative effects of climate change on water resources (decrease in P, R, and Sm). Decision makers could subsidize agricultural management practices that optimize the use of precipitation resources to compensate the possible loss of rainfed crop production and help cope with increasing risk of aridification. For instance, in Zambia (WOCAT, 2017) small Earth dams are being successfully used to collect runoff and provide irrigation and water for livestock.

Given the high uncertainty of model's projections and the weak agreement between models (especially regarding soil moisture simulations), this study does not aim to predict the impacts of hydroclimatic change on the socioeconomic activities of Africa. Rather, the aim of this study is to provide a general overview of the implications of future hydroclimatic change on water resources at the continental scale so as to provide guidance for large-scale policy decision making to support freshwater resources and agricultural development. Even if the Paris Agreement represent a potential desirable scenario to limit depletion of African water resources in key regions such as Northern and Southern Africa, its effectiveness is largely conditioned by the most developed countries outside of the continent. African countries can instead have more jurisdiction on local land management plans and thus directly contribute to preserve freshwater resources using sustainable agricultural practices. There are barriers to the implementation and spreading of the recommended agricultural management practices (e.g., mulching and rainwater harvesting), especially the financial costs in the implementation phase, higher labor required for some practices, and the high level of knowledge needed to properly implement and maintain these practices (Liniger et al., 2019). This paper delineates the potential use and the purpose of some of these practices to cope with hydroclimatic changes in the four key hydroclimate change regions of the African continent to inform policy and funding plans that could overcome these socioeconomic barriers and facilitate the implementation of such practices.

## 5. Conclusions

Hydroclimatic conditions following the Paris Agreement are likely to affect water resources in Africa less than the business as usual scenario, but in either case, African basins will consistently experience hydroclimatic change as outlined across the four groups here presented. This result highlights the potential of our hydroclimatic assessment to provide a roadmap to understand the major implications of hydroclimatic change on water resources and plan for effective and sustainable adaptation strategies at the regional level.

Climate change can induce unequal water availability in terms of precipitation and runoff, leading to reductions in irrigation potential, agricultural production, and possibly exacerbating conflicts over water resources in Northern and Southern Africa. On the other hand, some hydroclimatic changes can potentially provide more water to the key region of the Sahel, where water and land conservation practices such as water harvesting can promote agricultural production for the growing population. Sustainable land management can be extremely important to preserve and improve soil moisture and limit soil evaporation in regions with projected increase in PET/P, supporting food production under drier conditions (Southern and Northern Africa) and preventing soil loss and floods damage in wet regions (basins in tropical Africa).

However, more policies and funding are needed to make the spreading of these practices feasible and effective at larger scales.

#### Acknowledgments

This research was funded by the Swedish Research Council (VR, project 2015-06503) and the Swedish Research Council for Environment, Agricultural Sciences and Spatial Planning FORMAS (942-2015-740). JR and IF acknowledge funding from the European Research Council under EU H2020 'Earth resilience in the Anthropocene' (ERA) (grant no. ERC-2016-ADG 743080). We acknowledge the World Climate Research Programme's Working group on Coupled Modelling, which is responsible for CMIP, and we thank the climate modeling groups (listed in Table S1) for producing and making available their model output. The source code for the data processing and analysis developed in this study is freely available at [https://github.com/piemonteselugi/Africa\\_Future\\_Hydroclimate.git](https://github.com/piemonteselugi/Africa_Future_Hydroclimate.git).

#### References

- Arnell, N. W. (2004). Climate change and global water resources: SRES emissions and socio-economic scenarios. *Glob. Environ. Change, Climate Change*, 14, 31–52. <https://doi.org/10.1016/j.gloenvcha.2003.10.006>
- Asokan, S. M., Rogberg, P., Bring, A., Jarsjö, J., & Destouni, G. (2016). Climate model performance and change projection for freshwater fluxes: Comparison for irrigated areas in Central and South Asia. *Journal of Hydrology: Regional Studies*, 5, 48–65. <https://doi.org/10.1016/j.ejrh.2015.11.017>
- Asongu, S. A. (2013). How would population growth affect investment in the future? Asymmetric panel causality evidence for Africa. *African Development Review*, 25, 14–29. <https://doi.org/10.1111/j.1467-8268.2013.12010.x>
- Bain, L. E., Awah, P. K., Geraldine, N., Kindong, N. P., Siga, Y., Bernard, N., & Tanjeko, A. T. (2013). Malnutrition in sub-Saharan Africa: Burden, causes and prospects. *The Pan African Medical Journal*, 15. <https://doi.org/10.11604/pamj.2013.15.120.2535>
- Barrow, C. J. (1992). World atlas of desertification (United nations environment programme), edited by N. Middleton and D. S. G. Thomas. Edward Arnold, London, 1992. isbn 0 340 55512 2, £89.50 (hardback), ix + 69 pp. *Land Degradation and Development*, 3, 249–249. <https://doi.org/10.1002/ldr.3400030407>
- Bartle, A. (2002). Hydropower potential and development activities. *Energy Policy*, 30, 1231–1239. [https://doi.org/10.1016/S0301-4215\(02\)00084-8](https://doi.org/10.1016/S0301-4215(02)00084-8)
- Bhattacharjee, P. S., & Zaitchik, B. F. (2015). Perspectives on CMIP5 model performance in the Nile River headwaters regions. *International Journal of Climatology*, 35, 4262–4275. <https://doi.org/10.1002/joc.4284>
- Boko, M., Niang, I., Nyong, A., Vogel, C., Githeko, A., Medany, M., et al. (2007). Africa. In M. L. Parry, O. F. Canziani, J. P. Palutikof, P. J. van der Linden, & C. E. Hanson (Eds.), *Climate Change 2007: Impacts, Adaptation and Vulnerability. Contribution of Working Group II to the Fourth Assessment Report of the Intergovernmental Panel on Climate Change*, (pp. 433–467). Cambridge UK: Cambridge University Press.
- Bring, A., Asokan, S. M., Jaramillo, F., Jarsjö, J., Levi, L., Pietroni, J., et al. (2015). Implications of freshwater flux data from the CMIP5 multimodel output across a set of Northern Hemisphere drainage basins. *Earth's Future*, 3, 206–217. <https://doi.org/10.1002/2014EF000296>
- Budyko, M. I. (1963). *Evaporation under Natural Conditions*. Jerusalem: Israel Program for Scientific Translations.
- Budyko, M. I. (1971). *Climate and Life*, (p. 508). New York: Academic Press.
- Choudhury, B. (1999). Evaluation of an empirical equation for annual evaporation using field observations and results from a biophysical model. *Journal of Hydrology*, 216, 99–110. [https://doi.org/10.1016/S0022-1694\(98\)00293-5](https://doi.org/10.1016/S0022-1694(98)00293-5)
- Collier, P., Conway, G., & Venables, T. (2008). Climate change and Africa. *Oxford Review of Economic Policy*, 24, 337–353. <https://doi.org/10.1093/oxrep/grn019>
- Cook, B. I., Smerdon, J. E., Seager, R., & Coats, S. (2014). Global warming and 21st century drying. *Climate Dynamics*, 43, 2607–2627. <https://doi.org/10.1007/s00382-014-2075-y>
- Dai, A. (2011a). Drought under global warming: A review. *WIREs Climate Change*, 2, 45–65. <https://doi.org/10.1002/wcc.81>
- Dai, A. (2013). Increasing drought under global warming in observations and models. *Nature Climate Change*, 3, 52–58. <https://doi.org/10.1038/nclimate1633>
- Dai, A. (2011b). Characteristics and trends in various forms of the Palmer Drought Severity Index during 1900–2008. *Journal of Geophysical Research*, 116, D12115. <https://doi.org/10.1029/2010JD015541>
- Dile, Y. T., Karlberg, L., Daggupati, P., Srinivasan, R., Wiberg, D., & Rockström, J. (2016). Assessing the implications of water harvesting intensification on upstream–downstream ecosystem services: A case study in the Lake Tana basin. *Science of the Total Environment*, 542, 22–35. <https://doi.org/10.1016/j.scitotenv.2015.10.065>
- Donohue, R. J., McVicar, T. R., & Roderick, M. L. (2010). Assessing the ability of potential evaporation formulations to capture the dynamics in evaporative demand within a changing climate. *Journal of Hydrology*, 386, 186–197. <https://doi.org/10.1016/j.jhydrol.2010.03.020>
- Dore, M. H. I. (2005). Climate change and changes in global precipitation patterns: What do we know? *Environment International*, 31, 1167–1181. <https://doi.org/10.1016/j.envint.2005.03.004>
- Downing, T. E., Ringius, L., Hulme, M., & Waughray, D. (1997). Adapting to climate change in Africa. *Mitigation and Adaptation Strategies for Global Change*, 2, 19–44. <https://doi.org/10.1023/B:MITI.0000004663.31074.64>
- Easterly, W. (2009). How the millennium development goals are unfair to Africa. *World Development*, 37, 26–35. <https://doi.org/10.1016/j.worlddev.2008.02.009>
- Faramarzi, M., Abbaspour, K. C., Ashraf Vaghefi, S., Farzaneh, M. R., Zehnder, A. J. B., Srinivasan, R., & Yang, H. (2013). Modeling impacts of climate change on freshwater availability in Africa. *Journal of Hydrology*, 480, 85–101. <https://doi.org/10.1016/j.jhydrol.2012.12.016>
- Feng, S., & Fu, Q. (2013). Expansion of global drylands under a warming climate. *Atmospheric Chemistry and Physics*, 13, 10,081–10,094. <https://doi.org/10.5194/acp-13-10081-2013>
- Few, R., Gross-Camp, N., & Martin, A. (2014). Vulnerability, adaptation and mitigation in the forests of the Congo Basin: A critical investigation. *Cent. Int. For. Res.*
- Flint, L. E., & Flint, A. L. (2012). Downscaling future climate scenarios to fine scales for hydrologic and ecological modeling and analysis. *Ecological Processes*, 1, 2. <https://doi.org/10.1186/2192-1709-1-2>
- Fu, Q., & Feng, S. (2014). Responses of terrestrial aridity to global warming. *Journal of Geophysical Research: Atmospheres*, 119, 7863–7875. <https://doi.org/10.1002/2014JD021608>
- Gamo, M., Shinoda, M., & Maeda, T. (2013). Classification of arid lands, including soil degradation and irrigated areas, based on vegetation and aridity indices. *International Journal of Remote Sensing*, 34, 6701–6722. <https://doi.org/10.1080/01431161.2013.805281>
- Gerland, P., Raftery, A. E., Ševčíková, H., Li, N., Gu, D., Spoorenberg, T., et al. (2014). World population stabilization unlikely this century. *Science*, 346, 234–237. <https://doi.org/10.1126/science.1257469>
- Giorgi, F., Coppola, E., & Raffaele, F. (2014). A consistent picture of the hydroclimatic response to global warming from multiple indices: Models and observations. *Journal of Geophysical Research: Atmospheres*, 119, 11,695–11,708. <https://doi.org/10.1002/2014JD022238>

- Goulden, M., Conway, D., & Persechino, A. (2009). Adaptation to climate change in international river basins in Africa: A review/Adaptation au changement climatique dans les bassins fluviaux internationaux en Afrique: Une revue. *Hydrological Sciences Journal*, *54*, 805–828. <https://doi.org/10.1623/hysj.54.5.805>
- GRDC [WWW Document] (2017). wocat.net. [https://www.bafg.de/GRDC/EN/Home/homepage\\_node.html](https://www.bafg.de/GRDC/EN/Home/homepage_node.html) (accessed 1.16.17).
- Greve, P., Orłowski, B., Mueller, B., Sheffield, J., Reichstein, M., & Seneviratne, S. I. (2014). Global assessment of trends in wetting and drying over land. *Nature Geoscience*, *7*, 716–721. <https://doi.org/10.1038/ngeo2247>
- Gudmundsson, L., Greve, P., & Seneviratne, S. I. (2016). The sensitivity of water availability to changes in the aridity index and other factors—A probabilistic analysis in the Budyko space. *Geophysical Research Letters*, *43*, 6985–6994. <https://doi.org/10.1002/2016GL069763>
- Gudmundsson, L., Seneviratne, S. I., & Zhang, X. (2017). Anthropogenic climate change detected in European renewable freshwater resources. *Nature Climate Change*, *7*, 813–816. <https://doi.org/10.1038/nclimate3416>
- Hagemann, S., Chen, C., Clark, D. B., Folwell, S., Gosling, S. N., Haddeland, I., et al. (2013). Climate change impact on available water resources obtained using multiple global climate and hydrology models. *Earth System Dynamics*, *4*, 129–144. <https://doi.org/10.5194/esd-4-129-2013>
- Herrmann, S. M., Anyamba, A., & Tucker, C. J. (2005). Recent trends in vegetation dynamics in the African Sahel and their relationship to climate. *Global Environmental Change*, *15*, 394–404. <https://doi.org/10.1016/j.gloenvcha.2005.08.004>
- Hirabayashi, Y., Kanae, S., Emori, S., Oki, T., & Kimoto, M. (2008). Global projections of changing risks of floods and droughts in a changing climate. *Hydrological Sciences Journal*, *53*, 754–772. <https://doi.org/10.1623/hysj.53.4.754>
- Hoekstra, A. Y., Mekonnen, M. M., Chapagain, A. K., Mathews, R. E., & Richter, B. D. (2012). Global monthly water scarcity: Blue water footprints versus blue water availability. *PLoS ONE*, *7*, e32688. <https://doi.org/10.1371/journal.pone.0032688>
- Huntington, T. G. (2006). Evidence for intensification of the global water cycle: Review and synthesis. *Journal of Hydrology*, *319*, 83–95. <https://doi.org/10.1016/j.jhydrol.2005.07.003>
- Jägermeyr, J., Gerten, D., Schaphoff, S., Heinke, J., Lucht, W., & Rockström, J. (2016). Integrated crop water management might sustainably halve the global food gap. *Environmental Research Letters*, *11*, 025002. <https://doi.org/10.1088/1748-9326/11/2/025002>
- Jaramillo, F., & Destouni, G. (2014). Developing water change spectra and distinguishing change drivers worldwide. *Geophysical Research Letters*, *41*, 8377–8386. <https://doi.org/10.1002/2014GL061848>
- Jaramillo, F., & Destouni, G. (2015). Local flow regulation and irrigation raise global human water consumption and footprint. *Science*, *350*, 1248–1251. <https://doi.org/10.1126/science.aad1010>
- Kahinda, J. M., Lillie, E. S. B., Taigbenu, A. E., Taute, M., & Boroto, R. J. (2008). Developing suitability maps for rainwater harvesting in South Africa. *Phys. Chem. Earth Parts ABC*, *33*, 788–799. <https://doi.org/10.1016/j.pce.2008.06.047>
- Karl, T. R., & Knight, R. W. (1998). Secular trends of precipitation amount, frequency, and intensity in the United States. *Bulletin of the American Meteorological Society*, *79*, 231–241. [https://doi.org/10.1175/1520-0477\(1998\)079<0231:STOPAF>2.0.CO;2](https://doi.org/10.1175/1520-0477(1998)079<0231:STOPAF>2.0.CO;2)
- Kharin, V. V., Zwiers, F. W., Zhang, X., & Hegerl, G. C. (2007). Changes in temperature and precipitation extremes in the IPCC ensemble of global coupled model simulations. *Journal of Climate*, *20*, 1419–1444. <https://doi.org/10.1175/JCLI4066.1>
- Knutson, T. R., McBride, J. L., Chan, J., Emanuel, K., Holland, G., Landsea, C., et al. (2010). Tropical cyclones and climate change. *Nature Geoscience*, *3*, 157–163. <https://doi.org/10.1038/ngeo779>
- Koster, R. D., & Mahanama, S. P. (2012). Land Surface Controls on Hydroclimatic Means and Variability. *Journal of Hydrometeorology*, *13*, 1604–1620. <https://doi.org/10.1175/JHM-D-12-050.1>
- Liniger, H., Harari, N., van Lynden, G., Fleiner, R., de Leeuw, J., Bai, Z., & Critchley, W. (2019). Achieving land degradation neutrality: The role of SLM knowledge in evidence-based decision-making. *Environmental Science and Policy*, *94*, 123–134. <https://doi.org/10.1016/j.envsci.2019.01.001>
- Liniger, H., van Lynden, G., & Schwilch, G. (2002). Documenting field knowledge for better land management decisions: Experiences with WOCAT tools in local, national and global programs. In *Proceedings of 2002 ISCO Conference*, (pp. 167–259). Beijing: International Soil Conservation Organisation (ISCO).
- Maliva, R. G., & Missimer, T. M. (2012). *Arid Lands Water Evaluation and Management, Environmental Science*. Berlin Heidelberg: Springer.
- Mekonnen, M. M., & Hoekstra, A. Y. (2016). Four billion people facing severe water scarcity. *Science Advances*, *2*, e1500323. <https://doi.org/10.1126/sciadv.1500323>
- Milly, P. C. D., & Dunne, K. A. (2016). Potential evapotranspiration and continental drying. *Nature Climate Change*, *6*, 946–949. <https://doi.org/10.1038/nclimate3046>
- Milly, P. C. D., Dunne, K. A., & Vecchia, A. V. (2005). Global pattern of trends in streamflow and water availability in a changing climate. *Nature*, *438*, 347–350. <https://doi.org/10.1038/nature04312>
- Morsy, M., El-Sayed, T., & Ouda, S. A. H. (2016). Potential evapotranspiration under present and future climate. In *Management of Climate Induced Drought and Water Scarcity in Egypt*, (pp. 5–25). SpringerBriefs in Environmental Science. Springer International Publishing. [https://doi.org/10.1007/978-3-319-33660-2\\_2](https://doi.org/10.1007/978-3-319-33660-2_2)
- Nnoli, O. (1990). Desertification, refugees and regional conflict in West Africa. *Disasters*, *14*, 132–139. <https://doi.org/10.1111/j.1467-7717.1990.tb01054.x>
- Nohara, D., Kitoh, A., Hosaka, M., & Oki, T. (2006). Impact of climate change on river discharge projected by multimodel ensemble. *Journal of Hydrometeorology*, *7*, 1076–1089. <https://doi.org/10.1175/JHM531.1>
- Oweis, T., & Hachum, A. (2006). Water harvesting and supplemental irrigation for improved water productivity of dry farming systems in West Asia and North Africa. *Agricultural Water Management*, *80*, 57–73. <https://doi.org/10.1016/j.agwat.2005.07.004>
- Porkka, M., Gerten, D., Schaphoff, S., Siebert, S., & Kumm, M. (2016). Causes and trends of water scarcity in food production. *Environmental Research Letters*, *11*, 015001. <https://doi.org/10.1088/1748-9326/11/1/015001>
- Raferly, A. E., Zimmer, A., Frierson, D. M. W., Startz, R., & Liu, P. (2017). Less than 2 °C warming by 2100 unlikely. *Natural Climate Change*. <https://doi.org/10.1038/nclimate3352>
- Rockström, J., Williams, J., Daily, G., Noble, A., Matthews, N., Gordon, L., et al. (2017). Sustainable intensification of agriculture for human prosperity and global sustainability. *Ambio*, *46*, 4–17. <https://doi.org/10.1007/s13280-016-0793-6>
- Scheff, J., & Frierson, D. M. W. (2015). Terrestrial aridity and its response to greenhouse warming across CMIP5 climate models. *Journal of Climate*, *28*, 5583–5600. <https://doi.org/10.1175/JCLI-D-14-00480.1>
- Schewe, J., Heinke, J., Gerten, D., Haddeland, I., Arnell, N. W., Clark, D. B., et al. (2014). Multimodel assessment of water scarcity under climate change. *Proceedings of the National Academy of Sciences of the United States of America*, *111*, 3245–3250. <https://doi.org/10.1073/pnas.1222460110>

- Schuol, J., Abbaspour, K. C., Yang, H., Srinivasan, R., & Zehnder, A. J. B. (2008). Modeling blue and green water availability in Africa. *Water Resources Research*, 44, W07406. <https://doi.org/10.1029/2007WR006609>
- Seneviratne, S. I. (2012). Historical drought trends revisited: Climate science. *Nature*, 491, 338–339. <https://doi.org/10.1038/491338a>
- Sheffield, J., & Wood, E. F. (2008). Projected changes in drought occurrence under future global warming from multi-model, multi-scenario, IPCC AR4 simulations. *Climate Dynamics*, 31, 79–105. <https://doi.org/10.1007/s00382-007-0340-z>
- Sheffield, J., Wood, E. F., & Roderick, M. L. (2012). Little change in global drought over the past 60 years. *Nature*, 491, 435–438. <https://doi.org/10.1038/nature11575>
- Sherwood, S., & Fu, Q. (2014). A drier future? *Science*, 343, 737–739. <https://doi.org/10.1126/science.1247620>
- Siam, M. S., Demory, M.-E., & Eltahir, E. A. B. (2013). Hydrological cycles over the Congo and Upper Blue Nile Basins: Evaluation of general circulation model simulations and reanalysis products. *Journal of Climate*, 26, 8881–8894. <https://doi.org/10.1175/JCLI-D-12-00404.1>
- Swain, A. (2011). Challenges for water sharing in the Nile basin: changing geo-politics and changing climate. *Hydrological Sciences Journal*, 56, 687–702. <https://doi.org/10.1080/02626667.2011.577037>
- Sylla, M. B., Giorgi, F., Coppola, E., & Mariotti, L. (2013). Uncertainties in daily rainfall over Africa: assessment of gridded observation products and evaluation of a regional climate model simulation. *International Journal of Climatology*, 33, 1805–1817. <https://doi.org/10.1002/joc.3551>
- Taylor, K. E., Stouffer, R. J., & Meehl, G. A. (2011). An overview of CMIP5 and the experiment design. *Bulletin of the American Meteorological Society*, 93, 485–498. <https://doi.org/10.1175/BAMS-D-11-00094.1>
- Teng, J., Chiew, F.H., & Vaze, J. (2012). Will CMIP5 GCMs reduce or increase uncertainty in future runoff projections? *Hydrological Water Resour. Symp.* 2012 477.
- Thornthwaite, C. W. (1948). An approach toward a rational classification of climate. *Geographical Review*, 38, 55. <https://doi.org/10.2307/210739>
- Trail, P., Abaye, O., Thomason, W. E., Thompson, T. L., Gueye, F., Diedhiou, I., et al. (2016). Evaluating intercropping (living cover) and mulching (desiccated cover) practices for increasing millet yields in Senegal. *Agronomy Journal*, 108, 1742–1752. <https://doi.org/10.2134/agronj2015.0422>
- Trenberth, K. E., Dai, A., Rasmussen, R. M., & Parsons, D. B. (2003). The changing character of precipitation. *Bulletin of the American Meteorological Society*, 84, 1205–1218. <https://doi.org/10.1175/BAMS-84-9-1205>
- UNFCCC. (2015). Adoption of the Paris Agreement FCCC/CP/2015/L.9/Rev.1.
- Václavík, T., Lautenbach, S., Kuemmerle, T., & Seppelt, R. (2013). Mapping global land system archetypes. *Global Environmental Change*, 23, 1637–1647. <https://doi.org/10.1016/j.gloenvcha.2013.09.004>
- van der Velde, Y., Vercauteren, N., Jaramillo, F., Dekker, S. C., Destouni, G., & Lyon, S. W. (2014). Exploring hydroclimatic change disparity via the Budyko framework. *Hydrological Processes*, 28, 4110–4118. <https://doi.org/10.1002/hyp.9949>
- Vörösmarty, C. J., Green, P., Salisbury, J., & Lammers, R. B. (2000). Global water resources: Vulnerability from climate change and population growth. *Science*, 289, 284–288.
- Weiskel, P. K., Wolock, D. M., Zarriello, P. J., Vogel, R. M., Levin, S. B., & Lent, R. M. (2014). Hydroclimatic regimes: A distributed water-balance framework for hydrologic assessment, classification, and management. *Hydrology and Earth System Sciences*, 18, 3855–3872. <https://doi.org/10.5194/hess-18-3855-2014>
- Weltzin, J. F., Loik, M. E., Schwinning, S., Williams, D. G., Fay, P. A., Haddad, B. M., et al. (2003). Assessing the response of terrestrial ecosystems to potential changes in precipitation. *Bioscience*, 53, 941–952. [https://doi.org/10.1641/0006-3568\(2003\)053\[0941:ATROTE\]2.0.CO;2](https://doi.org/10.1641/0006-3568(2003)053[0941:ATROTE]2.0.CO;2)
- WOCAT. (2017). [WWW Document] wocat.net. URL <https://qcat.wocat.net/en/wocat/> (accessed 1.16.19).
- Yang, H., Yang, D., Lei, Z., & Sun, F. (2008). New analytical derivation of the mean annual water-energy balance equation. *Water Resources Research*, 44, W03410. <https://doi.org/10.1029/2007WR006135>
- You, L., Ringler, C., Wood-Sichra, U., Robertson, R., Wood, S., Zhu, T., et al. (2011). What is the irrigation potential for Africa? A combined biophysical and socioeconomic approach. *Food Policy*, 36, 770–782. <https://doi.org/10.1016/j.foodpol.2011.09.001>
- Zomer, R. J., Trabucco, A., Bossio, D. A., & Verchot, L. V. (2008). Climate change mitigation: A spatial analysis of global land suitability for clean development mechanism afforestation and reforestation. *Agriculture Ecosystems and Environment*, 126, 67–80. <https://doi.org/10.1016/j.agee.2008.01.014>

## Erratum

The acknowledgments have been updated since this paper was originally published. The authors have acknowledged funding from the European Research Council. This new version may be considered the version of record.